J Sol-Gel Sci Technol (2012) 63:235–241
DOI 10.1007/s10971-012-2720-z

ORIGINAL PAPER

Photophysics of aminobenzazole dyes in silica-based hybrid materials

Silvia Regina Grando · Fabiano da Silveira Santos · Márcia Russman Gallas · Tania Maria Haas Costa · Edilson Valmir Benvenutti · Fabiano Severo Rodembusch

Received: 11 November 2011 / Accepted: 18 February 2012 / Published online: 6 March 2012

Abstract In this work two aminobenzazole derivatives (5-AHBT and 5-AHBI) were dispersed in silica-based hybrid materials with different surface hydrophobicity, which were obtained by the sol–gel process using tetraethylorthosilicate as inorganic precursor and dimethyldimethoxysilane as organic precursor, with a molar percent of organic precursor changing from 0 to 50%. The photophysics of the obtained doped silica hybrid materials was investigated by means ultraviolet–visible diffuse reflectance and steady-state fluorescence emission spectroscopy in the solid state. The materials present absorption maxima located around 353 and 318 nm when doped with 5-AHBT and 5-AHBI, respectively. The red shifted absorption maxima of the 5-AHBT can be explained by the better electron delocalization allowed by the sulfur atom in relation to the nitrogen. The fluorescence emission spectra are located in the blue-green regions and the high Stokes shift indicates that the ESIPT mechanism occurs in the excited state for both dyes. The photophysical behavior of 5-AHBT shows that this dye is more affected by the matrix polarity due to specific interactions that take place in the ground state.

Keywords Photoactive matrix · Fluorescence · ESIPT · Hybrid xerogel materials

Electronic supplementary material The online version of this article (doi:10.1007/s10971-012-2720-z) contains supplementary material, which is available to authorized users.

S. R. Grando · F. da Silveira Santos · T. M. H. Costa · E. V. Benvenutti (✉)
LSS—Laboratório de Sólidos e Superfícies, Universidade Federal do Rio Grande do Sul, Avenida Bento Gonçalves, 9500, CP 15003, Porto Alegre-RS CEP 91501-970, Brazil
e-mail: benvenutti@iq.ufrgs.br

F. da Silveira Santos · F. S. Rodembusch (✉)
LNMO—Laboratório de Novos Materiais Orgânicos, Universidade Federal do Rio Grande do Sul, Avenida Bento Gonçalves, 9500, CP 15003, Porto Alegre-RS CEP 91501-970, Brazil
e-mail: rodembusch@iq.ufrgs.br

M. R. Gallas · T. M. H. Costa
LAPMA—Laboratório de Altas Pressões e Materiais Avançados, Universidade Federal do Rio Grande do Sul, Avenida Bento Gonçalves, 9500, CP 15003, Porto Alegre-RS CEP 91501-970, Brazil

1 Introduction

The development of organic–inorganic silica-based hybrid materials has received growing attention in the last decades. The possibility of producing new compounds that combine the properties of the organic and inorganic components has become increasingly attractive to material science research [1, 2]. These materials can present characteristics of the individual components as well as new unexpected properties, such as the increase in the ratio between the organic and inorganic precursor's amount in the sol–gel synthesis influences the characteristics of the final materials, such as hydrophobicity [3, 4]. To obtain these hybrid materials the sol–gel method is satisfactory, since allows dispersion of the components in nano or molecular scale, combining their physicochemical properties or producing new ones [5]. There is considerable interest in the sol–gel technology in the preparation of fluorescent materials for application in various systems such as solar collectors, lasers, sensors and materials for non-linear optics [6–9]. There has been a growing interest in the development of new fluorescent materials with good mechanical properties, thermal and chemical stability.

Organic–inorganic hybrid materials are considered to be good candidates to assemble such properties, lending themselves for applying in displays and lighting devices [6, 7]. Therefore, the characterization of physical and chemical properties of these hybrid materials doped with fluorescent dyes assumed a relevant role to determine possible applications [10–12]. The entrapment of fluorescent organic dyes into inorganic matrices obtained by sol–gel method leads to photoactive materials with attractive optical properties, since the silica xerogel matrix is a good host for the dyes due to its optical transparency and the possibility to disperse dyes at molecular level [2, 5, 13]. The benzazole dyes stand out among a large variety of organic fluorophores, due to a fluorescence emission with large Stokes shift ascribed to an intramolecular proton-transfer process (ESIPT) [3, 14] or an intramolecular charge transfer (ICT) in the excited-state [15–18], which can be tailored by the local polarity [14, 19]. In non-polar or aprotic solvents the enol-cis conformer is the most stable specie in the ground state, which on excitation undergoes ESIPT to form the keto tautomer, which gives rise to an emission with large stokes shift (T* emission). In protic or polar solvents, additional conformers are described and do not undergo ESIPT and are responsible for the short wavelength relaxation (N* emission) [14]. The conformational equilibrium in solution has been observed experimentally through the dual fluorescence emission with an emission at longer wavelengths ascribed to the excited keto tautomer, and a blue-shifted one due to conformational forms which presents a normal relaxation with Stokes shift lower than 5,834 cm^{-1} [20] (Fig. 1).

In this way, this work reports the synthesis and photophysical characterization by diffuse reflectance in the UV–Vis region and fluorescence emission in the solid-state of silica-based hybrid materials with different surface hydrophobicity containing dispersed fluorescent organic dyes based on aminobenzazoles derivatives as potential materials for optical sensors.

2 Methods

2.1 Materials

Tetraethylorthosilicate (TEOS) (Reagent Grade 98%), dimethoxydimethylsilane (DDMS) (85%) and pyrene were purchased from Aldrich, absolute ethanol (Merck) and fluoridric acid 40% (Synth), which was used as catalyst in the sol–gel synthesis, were used as received. The fluorescent dyes 2-(5′-amino-2′-hydroxyphenyl)benzothiazole (5-AHBT) and 2-(5′-amino-2′-hydroxyphenyl)benzimidazole (5-AHBI) (Fig. 2) were synthesized according to the literature [14].

2.2 Synthesis of the doped silica hybrid materials

Two fluorescent aminobenzazole derivatives (5-AHBT) and (5-AHBI) were dispersed in the silica hybrid materials with different surface hydrophobicity, which were obtained by the sol–gel method. The samples were prepared using tetraethylorthosilicate (TEOS) as inorganic precursor and dimethyldimethoxysilane (DDMS) as organic precursor, with a molar percent of organic precursor changing from 0 to 50%. The samples were prepared by addition of 5.0 mL of an ethanolic solution of dyes (5.0×10^{-4} $molL^{-1}$) to the molecular precursors under stirring at room

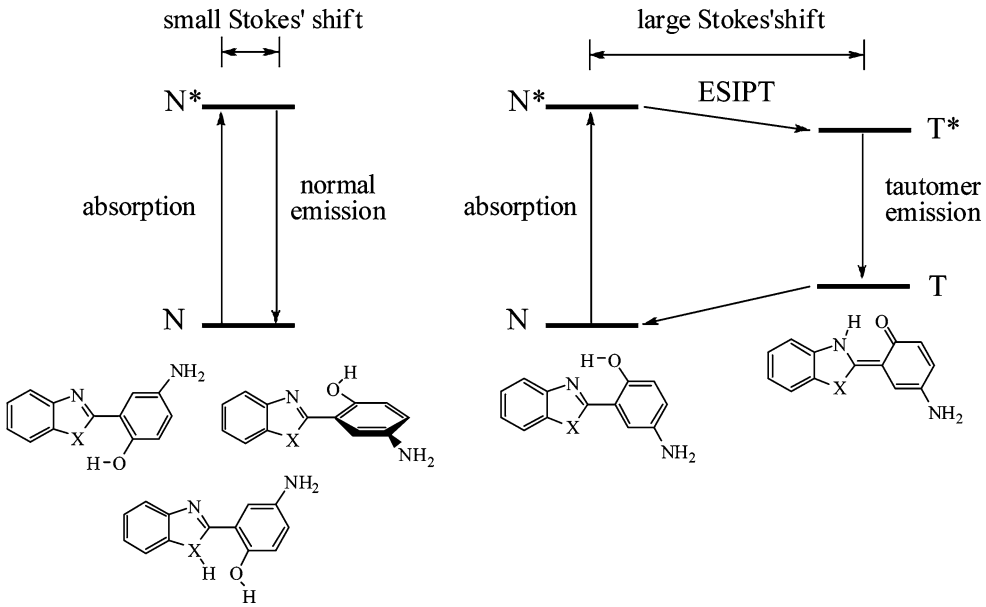

Fig. 1 ESIPT mechanism of the aminoderivatives, where X = S or NH

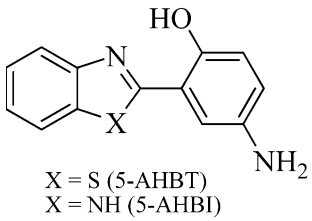

Fig. 2 Chemical structure of the fluorescent dyes (5-AHBT) and (5-AHBI)

temperature. The total quantity of silicon was maintained constant as 2.2×10^{-2} mol in all samples. Afterward, it was added under stirring 0.1 mL of aqueous HF 40% and water, according to Table 1.

The solutions were cast in Teflon plates and stored at ambient conditions for about a month for gelation and solvent evaporation. The resulting monoliths were comminuted. Moreover, for each synthesized sample it was also prepared a reference sample, without the dyes addition. The process of doped silica hybrid materials synthesis is presented in Scheme 1. For each synthesized sample it was also prepared a silica hybrid material without the dyes addition. These samples were impregnate with pyrene fluorescent probe using an ethanolic solution 10^{-6} molL^{-1} to evaluate the polarity of the silica hybrid materials.

2.3 Characterization

The UV–Vis diffuse reflectance spectra were measured with a spectrophotometer Shimadzu UV2450PC using an ISR-2200 integrating sphere attachment. The experiments were performed at room temperature and the baseline in the solid-state was obtained using $BaSO_4$ (Wako Pure Chemical Industries, Ltd.). Fluorescence spectra were measured with a Shimadzu spectrofluorometer RF5301. For these experiments the obtained materials were treated as powder. Powdered samples of the silica hybrid materials were analyzed by transmission FTIR spectroscopy using the KBr technique. The samples and the KBr were previously dried at 120 °C. The spectra were obtained in Shimadzu equipment model prestige 21 with 4 cm^{-1} of resolution and 40 scans.

Table 1 Synthesis parameters of the obtained doped materials MAHBT and MAHBI

Dye	Doped materials	DDMS (molar %)	Water (mL)
5-AHBT	MAHBT	0	1.6
	MAHBT10	10	1.5
	MAHBT30	30	1.3
	MAHBT50	50	1.2
5-AHBI	MAHBI	0	1.6
	MAHBI10	10	1.5
	MAHBI30	30	1.3
	MAHBI50	50	1.2

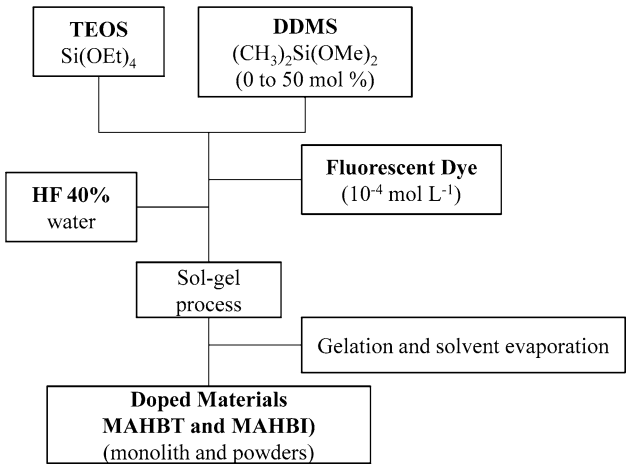

Scheme 1 Sol–gel process of the photoactive hybrid materials preparation

3 Results and discussions

3.1 FTIR and micropolarity analysis

Infrared analysis of the silica hybrid materials (S) is presented in Fig. 3. For the sample prepared with 0% of DDMS (S0) it is possible to observe a typical silica spectrum with a large band with maximum near 1,090 cm^{-1} that is attributed to stretching vibration of Si–O bonds and

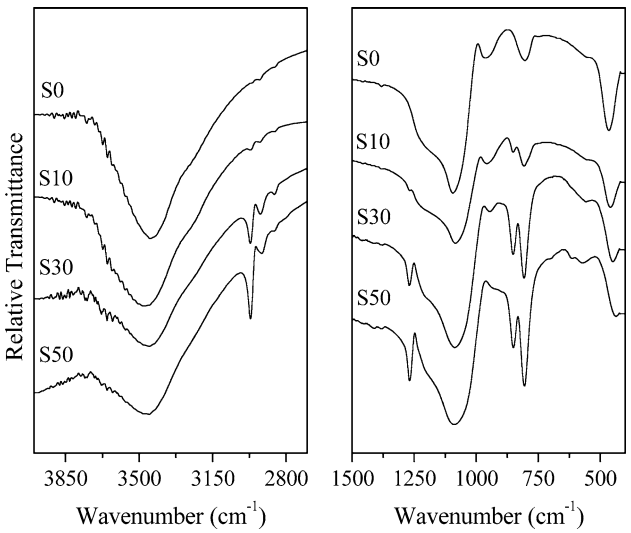

Fig. 3 FTIR spectra of the set of silica hybrid materials (S0–S50) obtained at room temperature

a band with maximum at 805 cm^{-1} due to the bending Si–O–Si bonds [21–23]. For the sample prepared with 10% DDMS (S10), in addition to the characteristic silica features, new bands can be observed, which are related to the hybrid material formation. The main C–H stretching band of methyl groups appears at 2,970 cm^{-1} [24], where its intensity increase with the increasing of the organic content (from 10 to 50% DDMS). It is worth mentioning that the band located around 1,270 cm^{-1} is used to characterize the Si–CH_3 group, assigned as methyl deformation [24, 25]. The bands located at 850 and 800 cm^{-1}, which are related to methyl rocking and Si–C stretching [24, 25] corroborates with the increase of the DDMS in the hybrid material [24, 25]. The intensity of all the bands related to methyl groups bonded to silicon increases from S10 to S50. Additionally, it can be observed a shoulder near 950 cm^{-1}, due to the Si–O stretching of silanol groups, where its intensity decreases with the increasing of the organic content.

As already presented in the literature, the increase of the organic contend into the silica matrix can change the local polarity of the hybrid material [3]. In order to evaluate the micropolarity of the obtained silica hybrid materials, pyrene was used as probe [4, 26, 27]. An excitation wavelength located at 337 nm results in vibronic bands in the pyrene emission spectrum. The intensity ratio of two bands (I_1 and I_3, $\lambda_{em} = 372$ and 382 nm, respectively) can be related to the local hydrophobicity of probe surrounding. The increasing in the I_3/I_1 ratio indicates an increasing in the hydrophobicity [4, 26, 27]. The spectra of the samples are presented in the Electronic Supplementary Material (Figure ESM1). It could be observed an increasing in the I_3/I_1 ratio from S0 to S50 (0.63–0.98) indicating an increasing in the matrix surface hydrophobicity, as expected.

3.2 DRUV spectroscopy

Figure 4 presents the normalized diffuse reflectance UV–Vis absorbance of the obtained doped silica hybrid materials. The relevant UV–Vis data are summarized in Table 2. Absorption band maxima located around 353 and 318 nm could be observed for the silica hybrid materials doped with 5-AHBT and 5-AHBI, respectively. The red shifted absorption maxima of the 5-AHBT, in despite of the 5-AHBI, can be explained by the better electron delocalization allowed by the sulfur atom in relation to the nitrogen [14, 28].

In the doped silica hybrid materials using the 5-AHBI it could not be observed a shift on the absorption maxima with the increase of the organic content into the silica matrix. This demonstrates that the electronic structure of this fluorophore was not significantly perturbed in the ground state with the introduction of the DDMS in the silica hybrid material. The same photophysical behavior could be observed for this dye in solution, where the absorption maxima do not shift in increasing the solvent polarity [14]. However, the silica hybrid materials prepared with the dye 5-AHBT presented a blue shift for the absorption maxima with the increasing the matrix polarity. The blue shift can be attributed to the partial breaking of the intramolecular hydrogen bond between the hydroxyl group and the azolic nitrogen as a result of competition with the intermolecular hydrogen bond formation with the silanol moieties [19]. Additional hydrogen bonds can occur between the Si–OH and the amino groups, which are presented in the structure, and seems to better stabilize the dye in the ground state. It is worth mentioning that the electronic spectra of this dye is quite different from those obtained in solution of dichloromethane, ethanol and acetonitrile [14], where a red shifted on the absorption maxima was reported for 5-AHBT increasing the solvent polarity. Additionally, in solution the dyes 5-AHBT and 5-AHBI presents an intense absorption bands at 280–310 nm, which are absent in the solid state and can be associated to a difference of planarity of the dyes [29]. A non-planar structure does not allow a more effective electronic delocalization among the two π systems (aminophenolic and benzazolic rings). In this way, the photoactive dyes showed to present a higher planarity in the silica hybrid material than in solution. The Stokes shift and the evidence of ESIPT emission corroborates with this affirmation and will be discussed in this work. To better compare the solid-state results, the spectra of the photoactive dyes in solution are presented in the Electronic Supplementary Material (Figures ESM2 and ESM3).

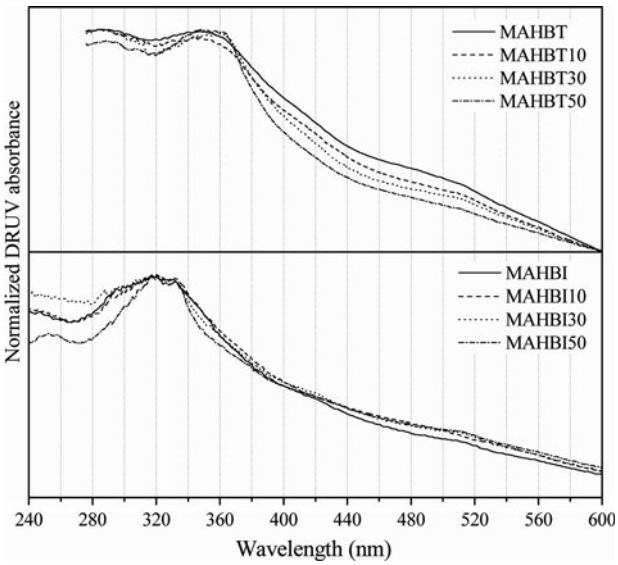

Fig. 4 DRUV spectra of the doped silica hybrid materials

Table 2 Solid-state UV–Vis absorption and fluorescence emission data of the doped materials

Dye	Doped materials	λ_{abs} (nm)	λ_{em} (nm)		$\Delta\lambda_{ST}$ (nm/cm^{-1})
5-AHBT	MAHBT	348	496		148/8,574
	MAHBT10	347	512		165/9,287
	MAHBT30	354	531		177/9,416
	MAHBT50	353	533		180/9,567
Dye	Doped materials	λ_{abs} (nm)	λ_{em} (nm)		$\Delta\lambda_{ST}$ (nm/cm^{-1})
			N*	T*	
5-AHBI	MAHBI	317	380	479	162/10,669
	MAHBI10	320	375	458	138/9,416
	MAHBI30	317	378	465	148/10,040
	MAHBI50	316	379	469	153/10,324

3.3 Fluorescence emission spectroscopy

The normalized fluorescence emission spectra of the doped silica hybrid materials are presented in Fig. 5. The spectra were obtained using the absorption maxima as the excitation wavelengths. The relevant data is presented in Table 2. In all doped silica hybrid materials, the emission spectra of the 5-AHBI present one main band located at around 468 nm, with a Stokes shift of ca. 115 nm, ascribed to an ESIPT emission (T* emission) and a small blue-shifted band located at around 378 nm (normal emission, N*, Stokes shift ca. 60 nm). No significant shift could be observed in the emission bands varying the silica matrix polarity. This photophysical behavior was already observed for these dyes and is related to a conformational equilibrium in the ground state [14], where in nonpolar and aprotic environment an enol-cis conform is the most stable conformer in the ground state. This conformer on excitation undergoes ESIPT to form the keto tautomer, which gives rise to an emission with large Stokes shift. In polar and protic media, other conformers, which do not undergo ESIPT, are responsible for a normal emission with shorter wavelength [30–32].

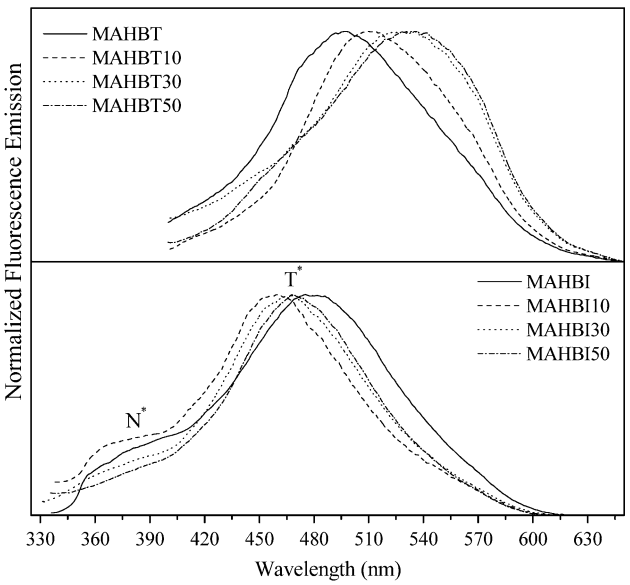

Fig. 5 Fluorescence emission spectra of the doped silica hybrid materials

On the other hand, the dye 5-AHBT presents a fluorescence emission tailored by the polarity of the hybrid material, with a emission maxima varying from 496 to 533 nm with the increase of the organic contend (% DDMS) in the silica material (decrease of polarity). Usually, a red shift in the emission maxima is associated with changes in the excited state charge distribution as compared to that in the ground state, related with a intramolecular charge transfer (ICT) state [33, 34]. In a more polar environment, the species with charge separation may become the lowest energy state. In a non-polar solvent the species without charge separation, the so-called locally excited state, may have the lowest energy. However, the photophysical behavior observed for 5-ABHT in the silica hybrid material is the opposite, where the less polar environment seems to better stabilize the dye in the excited state. The role of the environment polarity is not only to lower the energy of the excited state due to general electrostatic interactions, but also to govern which state has the lowest energy [35].

The observed Stokes shift of 5-AHBT is related to the ESIPT mechanism in all silica hybrid materials (ca. 135 nm) and the fluorescence emission location, tailored by the organic content (% DDMS), discard the ICT state in the excited state for this dye. In this way, the blue shift of the emission spectra increasing the matrix polarity can also be attributed to a better stabilization of 5-AHBT in the ground state (lower S_0), due to specific hydrogen bonds between the azolic nitrogen, the amino and the hydroxyl moieties present in this dye. The difference of the photophysical behavior of the dye 5-AHBI, almost constant absorption and emission maxima changing the matrix

polarity, may reside in an annular tautomerism, which involves the movement of a proton between two annular nitrogen atoms [36, 37]. This type of prototropism would modify the conjugation length of the 5-AHBI, since now the H of the NH group would be delocalized between the nitrogens of the benzimidazolic ring, enabling simultaneously more than one conjugation path. We identify it as a manifestation of a resonance-assisted hydrogen bond (RAHB), which leads to a greater electronic delocalization in the benzimidazolic ring [38–40].

4 Conclusions

Photoactive hybrid materials were obtained by dispersion of two fluorescent aminobenzazole dyes in silica matrix with different surface hydrophobicity, which were prepared by the sol–gel process using tetraethylorthosilicate and dimethyldimethoxysilane with a molar percent changing from 0 to 50%. The hybrid materials present absorption maxima located around 353 and 318 nm when doped with 5-AHBT and 5-AHBI, respectively. The red shifted absorption maxima of the 5-AHBT in despite of the 5-AHBI was related to the better electron delocalization allowed by the sulfur atom in relation to the nitrogen. The fluorescence emission spectra of the photoactive matrices are located in the blue-green regions and the high Stokes shift indicates that the ESIPT mechanism occurs in the excited state.

The 5-AHBI seems not to be affected by the matrix polarity, where any significant shift in the absorption or emission could be detected. The fluorescence emission location of 5-AHBT tailored by the organic content discard the ICT state in the excited state. The blue shifted emission spectra with the increasing of the matrix polarity can be attributed to a better stabilization of 5-AHBT in the ground state, due to specific hydrogen bonds between the dye and the matrix. The difference of the photophysical behavior of the dye 5-AHBI in despite the 5-AHBT may reside in an annular tautomerism, which leads to a greater electronic delocalization in the benzimidazolic ring, which do not allow an effective interaction in the ground state of the hydrogen bond and the silanol groups of the silica matrix.

Acknowledgments The authors thank Conselho Nacional de Desenvolvimento Científico e Tecnológico, Coordenação de Aperfeiçoamento de Pessoal de Nível Superior and Fundação de Amparo à Pesquisa do Estado do Rio Grande do Sul for financial support and Instituto Nacional de Inovação em Diagnósticos para a Saúde Pública.

References

1. Avnir D (1995) Organic chemistry within ceramic matrices: doped sol–gel materials. Acc Chem Res 28:328–334
2. Mehdi A, Reye C, Corriu R (2011) From molecular chemistry to hybrid nanomaterials. Design and functionalization. Chem Soc Rev 40:563–574
3. Grando SR, Pessoa CM, Gallas MR, Costa TMH, Rodembusch FS, Benvenutti EV (2009) Modulation of the ESIPT emission of benzothiazole type dye incorporated in silica-based hybrid materials. Langmuir 25:13219–13223
4. Keeling-Tucker T, Brennan JD (2001) Fluorescent probes as reporters on the local structure and dynamics in sol–gel-derived nanocomposite materials. Chem Mater 13:3331–3350
5. Brinker CJ, Scherer GW (1990) Sol–gel science. Acad Press, NewYork
6. Lacatusu I, Badea N, Bojin D, Iosub S, Meghea A (2009) Novel fluorescence nano structured materials obtained by entrapment of an ornamental bush extract in hybrid silica glass. J Sol–gel Sci Technol 51:84–91
7. Nedelcev T, Krupa I, Hrdlovic P, Kollar J, Chorvat D, Lacik I (2010) Silica hydrogel formation and aging monitored by pyrene-based fluorescence probes. J Sol–gel Sci Technol 55:143–150
8. Unger B, Rurack K, Muller R, Resch-Genger U, Buttke K (2000) Effects of the sol–gel processing on the fluorescence properties of laser dyes in tetraethoxysilane derived matrices. J Sol–gel Sci Technol 19:799–802
9. Reisfeld R (2001) Prospects of sol–gel technology towards luminescent materials. Opt Mater 16:1–7
10. Cui YJ, Yu JC, Gao JK, Wang ZY, Qian GD (2009) Synthesis and luminescence behavior of inorganic-organic hybrid materials covalently bound with pyran-containing dyes. J Sol–gel Sci Technol 52:362–369
11. Hoffmann HS, Stefani V, Benvenutti EV, Costa TMH, Gallas MR (2011) Fluorescent silica hybrid materials containing benzimidazole dyes obtained by sol–gel method and high pressure processing. Mater Chem Phys 126:97–101
12. Wallington SA, Pilon C, Wright JD (1997) Sol–gel composites for optical sensing of solvents. J Sol–gel Sci Technol 8: 1127–1132
13. Sanz-Menez N, Monnier V, Colombier I, Baldeck PL, Irie M, Ibanez A (2011) Photochromic fluorescent diarylethene nanocrystals grown in sol–gel thin films. Dyes Pigm 89:241–245
14. Rodembusch FS, Leusin FP, Campo LF, Stefani V (2007) Excited state intramolecular proton transfer in amino 2-(2′-hydroxyphenyl)benzazole derivatives: effects of the solvent and the amino group position. J Lumin 126:728–734
15. Etaiw SE-DH, Fayed TA, Saleh NZ (2006) Photophysics of benzazole derived push-pull butadienes: a highly sensitive fluorescence probes. J Photochem Photobiol A Chem 177:238–247
16. Fayed TA, Etaiw SE-DH, Khatab HM (2005) Excited state properties and acid-base equilibria of trans-2-styrylbenzoxazoles. J Photochem Photobiol A Chem 170:97–103
17. Yoshihara T, Druzhinin SI, Zachariasse KA (2004) Fast intramolecular charge transfer with a planar rigidized electron donor/acceptor molecule. J Am Chem Soc 126:8535–8539
18. Santos FS, Costa TMH, Stefani V, Gonçalves PFB, Descalzo RR, Benvenutti EV, Rodembusch FS (2011) Synthesis, characterization, and spectroscopic investigation of benzoxazole conjugated Schiff bases. J Phys Chem A 115:13390–13398
19. Dey JK, Dogra SK (1991) Solvatochromism and prototropism in 2-(aminophenyl) benzothiazoles. Bull Chem Soc Jpn 64: 3142–3152
20. Santra S, Dogra SK (1998) Excited-state intramolecular proton transfer in 2-(2′-aminophenyl) benzimidazole. Chem Phys 226: 285–296
21. Costa TMH, Gallas MR, Benvenutti EV, da Jornada JAH (1997) Infrared and thermogravimetric study of high pressure consolidation in alkoxide silica gel powders. J Non-Cryst Solids 220:195–201

22. Almeida RM, Pântano CG (1990) Structural investigation of silica-gel films by infrared-spectroscopy. J Appl Phys 68:4225–4232
23. Wood DL, Rabinovich EM (1989) Study of alkoxide silica-gels by infrared-spectroscopy. Appl Spectrosc 43:263–267
24. Colthup NB, Daly LH, Wiberley SE (1975) Introduction to infrared and raman spectroscopy. Academic Press, New York
25. Bellamy LJ (1975) The infrared spectra of complex molecules. Chapman and Hall, New York
26. Baker GA, Pandey S, Maziarz EP, Bright FV (1999) Toward tailored xerogel composites: local dipolarity and nanosecond dynamics within binary composites derived from tetraethylorthosilane and ORMOSILs, oligomers or surfactants. J Sol–gel Sci Technol 15:37–48
27. Christoff M, Silveira NP, Samios D (2001) Fluorescence and light scattering studies on the aggregation of sodium cholate in the presence of low molecular weight poly (ethylene oxide). Langmuir 17:2885–2888
28. Campo LF, Sanchez M, Stefani V (2006) Spectral properties of amorphous silica (SiO_2) and mesoporous structured silicates (MCM-41 and ITQ-6) functionalized with ESIPT chromophores. J Photochem Photobiol A Chem 178:26–32
29. Douhal A, Amat-Guerri F, Lillo MP, Acuña AU (1994) Proton-transfer spectroscopy of 2-(2′-hydroxyphenyl)imidazole and 2-(2′-hydroxyphenyl) benzimidazole dyes. J Photochem Photobiol A Chem 78:127–138
30. Vazquez SR, Rodriguez MCR, Mosquera M, Rodriguez-Prieto F (2007) Excited-state intramolecular proton transfer in 2-(3′-hydroxy-2′-pyridyl) benzoxazole. Evidence of coupled proton and charge transfer in the excited state of some o-hydroxyarylbenzazoles. J Phys Chem A 111:1814–1826
31. Mordzinski A, Grabowska A, Kuhnle W, Krowczynski A (1983) Intramolecular single and double proton-transfer in benzoxazole derivatives. Chem Phys Lett 101:291–296
32. Mordzinski A (1988) Polyethylene as a medium for eliminating the solvent perturbation in intramolecular proton-transfer systems. Chem Phys Lett 150:254–258
33. Zachariasse KA, Grobys M, von der Haar T, Hebecker A, Il'ichev YV, Jiang Y-B, Morawski O, Kühnle W (1996) Intramolecular charge transfer in the excited state. Kinetics and configurational changes. J Photochem Photobiol A Chem 102:59–70
34. Grabowski ZR, Rotkiewicz K, Rettig W (2003) Structural changes accompanying intramolecular electron transfer: focus on twisted intramolecular charge-transfer states and structures. Chem Rev 103:3899–4031
35. Lakowicz JR (2006) Solvent and environmental effects. Principles of fluorescence spectroscopy. Springer, New York, NY
36. Lumbroso H, Liegeois C, Pappalardo GC, Grassi A (1982) A theoretical and experimental dipole-moment study of annular tautomerism in tetrazole. J Mol Struct 82:283–294
37. Ogretir C, Yarligan S, Berber H, Arslan T, Topal S (2003) A theoretical study of substituent effects on tautomerism of 2-hydroxybenzimidazoles. J Mol Model 9:390–394
38. Rodembusch FS, Buckup T, Segala M, Tavares L, Correia RRB, Stefani V (2004) First hyperpolarizability in a new benzimidazole derivative. Chem Phys 305:115–121
39. Grabowski SJ (2001) An estimation of strength of intramolecular hydrogen bonds—ab initio and AIM studies. J Mol Struct 562: 137–143
40. Gilli P, Bertolasi V, Pretto L, Ferretti V, Gilli G (2004) Covalent versus electrostatic nature of the strong hydrogen bond: discrimination among single, double, and asymmetric single-well hydrogen bonds by variable-temperature X-ray crystallographic methods in beta-diketone enol RAHB systems. J Am Chem Soc 126:3845–3855